Three-dimensional multifluid simulation of the plasma interaction at Titan

D. Snowden,[1] R. Winglee,[1] C. Bertucci,[2] and M. Dougherty[2]

Received 8 March 2007; revised 6 September 2007; accepted 28 September 2007; published 29 December 2007.

[1] Using a three-dimensional multifluid simulation, we demonstrate the importance of ion gyroradius and heavy ion effects when characterizing Titan's plasma interaction with the Kronian magnetosphere. Ion gyroradius and heavy ion effects drastically change the mass loading and magnetic field draping at Titan. We find that the large ion gyroradius of picked up ionospheric species results in an extension of the ionosphere and therefore the mass loading and magnetic pileup region on the anti-Saturn side of Titan. Also, the additional thermal pressure provided by heavy ion cyclotron motion near Titan causes boundary layer currents to form at higher altitudes. The Saturn-facing side of Titan's ionosphere experiences both magnetic shielding from the incident plasma at lower altitudes and additional heating due to the acceleration of heavy ions in the ionosphere. Finally, we find that well-confined heavy ion beams form on the anti-Saturn side of Titan's magnetosphere and extend more than three Titan radii from Titan's main ion tail. The location of this ion beam is dependent on the Kronian field orientation, and we find that during the TA, TB, and T3 encounters, the bulk of the ion beam was located below Titan's equatorial plane. We also find that for a single set of incident conditions, good agreement with Cassini magnetometer data from the TA, TB, and T3 encounters is obtained with the ion loss rate similar to that measured by Cassini during the TA encounter.

Citation: Snowden, D., R. Winglee, C. Bertucci, and M. Dougherty (2007), Three-dimensional multifluid simulation of the plasma interaction at Titan, *J. Geophys. Res.*, *112*, A12221, doi:10.1029/2007JA012393.

1. Introduction

[2] Titan orbits at 20 Saturn radii, near the outskirts of Saturn's magnetosphere where it encounters a mix of plasma from the rings, the inner moons, Saturn's ionosphere, ions lost from its own ionosphere, and the solar wind. Similar to the induced magnetospheres of Venus and Mars, the Kronian plasma interacts with Titan's ionosphere causing the plasma to be deflected around Titan. This interaction forms a cavity region and a wake of outflowing plasma [*Wolf and Neubauer*, 1982].

[3] Measurements obtained during Cassini's first flyby of Titan, known as TA, confirmed the prediction that the large ion gyroradii of incident species would be an important factor in describing the plasma flow near Titan. Results from this flyby indicated that the dominant Kronian ions near Titan's orbit are H^+, H_2^+, N^+/CH_2^+, and O^+/CH_4^+ flowing at $\sim$110 km s^{-1} [*Hartle et al.*, 2006]. Magnetometer data measured the magnitude of Saturn's magnetic field at Titan's orbit to be about 5 nT. The gyroradii of the incident species was $\sim$400 km for protons and $\sim$6400 km for O^+/CH_4^+ ions. Therefore the heavy ions near Titan's orbit have gyroradii that are on the order of the diameter of Titan (5150 km). *Hartle et al.* [2006] analyzed the ion mass spectrometer data from both the Cassini TA flyby and the Voyager 1 flyby that took place on 12 November 1980. They found a "clearing area" around Titan with a size equal to the incident ions gyrodiameter formed in which the density of the incident species was greatly reduced due to collisions with Titan's atmosphere. They attributed the "clearing area" to the large ion gyroradius of the incoming species.

[4] In the T5 flyby, which encountered the night side of Titan's ionosphere, $HCNH^+$ was found to be the most abundant ionospheric species along with $C_2H_5^+$, CH_5^+, and $C_3H_5^+$ and heavy ion species $C_7H_7^+$ and $C_3H_3N^+$ [*Cravens et al.*, 2006]. The magnetic field in the magnetic pileup region was measured to be $\sim$10 nT [*Backes et al.*, 2005]. Therefore ions in Titan's ionosphere that are "picked up" by the $\vec{v} \times \vec{B}$ field of the flowing Kronian plasma have ion gyroradii on the order of hundred of kilometers in the mass loaded region and $\sim$7000 km in the ambient Kronian conditions. Looking down on the orbital plane of Saturn, ions will drift in a clockwise direction. The rotation means that ions accelerated on the side of Titan's ionosphere facing Saturn will drift back into the ionosphere where they are likely to be reincorporated, while ions accelerated on the anti-Saturn side will drift away from Titan's ionosphere. The inflation of Titan's outflow and mass loading region on the anti-Saturn side has been observed in Voyager and Cassini

[1]Department of Earth and Space Sciences, University of Washington, Seattle, Washington, USA.
[2]Space and Atmospheric Physics Group, Imperial College, London, UK.

0148-0227/07/2007JA012393

plasma and magnetometer data [*Wahlund et al.*, 2005; *Sittler et al.*, 2005].

[5] The change in illumination of Titan's ramside ionosphere as Titan orbits around Saturn's is another characteristic of the plasma interaction that must be considered. Photoionization is thought to be the dominant ionization source [*Cravens et al.*, 1992; *Keller et al.*, 1998]. Therefore the density of Titan's ramside ionosphere could change significantly with the solar zenith angle. The formation of a current layer in the ionosphere is dependent on the density of ions in Titan's upper atmosphere [*Sittler et al.*, 2005]. Therefore the location of the Sun-Titan line relative to the incident plasma flow could have an effect on the extent of the mass loaded region where ion pickup occurs [*Blanc et al.*, 2002].

[6] Both magnetohydrodynamic (MHD) and hybrid models have been developed to study the Titan interaction. Three-dimensional MHD models of Titan's plasma interaction by *Ledvina and Cravens* [1998], *Kabin et al.* [1999], and *Backes et al.* [2005] recreated expected features of an induced magnetosphere including a magnetic pileup region and a two-lobe tail structure. *Ledvina and Cravens* [1998] modeled Titan's interaction for several different plasma conditions and found that the nature of Titan's plasma interaction strongly depends on the incident conditions. *Kabin et al.* [1999] compared the results of their model with Voyager magnetometer data. Although, their model was able to recreate the basic form of the Voyager data the author cautioned that details of the interaction are likely incorrect because the lack of ion gyroradius effects. *Backes et al.* [2005] was able to recreate portions of the initial Titan flyby. Most recently, a comprehensive MHD model by *Ma et al.* [2006] showed reasonable agreements with magnetometer and plasma data from the TA and TB encounters. These models are useful in giving a picture of the general morphology of Titan's induced magnetosphere. However, we show that ion cyclotron and heavy ion effects that cannot be included in MHD simulations are a significant part of the Titan interaction.

[7] Hybrid models that account for individual ion gyromotion have confirmed the significance of finite gyroradius effects. Three-dimensional hybrid models of the Titan interaction have been provided by *Brecht et al.* [2000] and *Sillanpää et al.* [2006]. *Brecht et al.*'s [2000] three-dimensional hybrid model confirmed that Titan's induced magnetotail is highly asymmetric and that the size of Titan's magnetotail is dominated by the large ion gyroradius of heavy ions from Titan's ionosphere. However, solving for the movement of individual particles is computationally intensive. Therefore hybrid models are typically limited in simulation size and/or resolution. In the described hybrid model the spatial resolution is about 1000 km near Titan, which is too large to properly resolve smaller features in Titan's ionosphere such as the formation of current layers or the density variation due to the changing solar zenith angle.

[8] This paper introduces a three-dimensional multifluid simulation of the plasma interaction at Titan. The multifluid method is well suited to study Titan because it includes ion gyroradius effects of individual ion species and is computationally simple enough to obtain high resolution ($\sim$125 km). We show that finite gyroradius effects lead to important asymmetries in heating of Titan's ionosphere, mass loading, and ion outflow. The asymmetries in the interaction at Titan are important to understanding Titan's impact on the dynamics of Saturn's magnetosphere and how the incident Kronian plasma and fields affects Titan's dense atmosphere.

2. Model

2.1. Multifluid Equations

[9] The standard way to include ion cyclotron effects and different ion species is to use a hybrid simulation, which solves for the dynamics of individual ion particles and fluid electrons. The disadvantage of this method is that a large number of particles must be included to accurately represent the ion distribution in each cell; this limits simulations in size and/or resolution. The multifluid approach is similar but it simplifies the hybrid approach by simulating each ion species as a fluid. The fluid approximation allows the multifluid method the ability to obtain good resolution with modest computing resources. This approach has been used successfully to model the minimagnetospheres at Mars [*Harnett and Winglee*, 2003], the magnetosphere around Ganymede [*Paty and Winglee*, 2004], the induced magnetosphere around Pluto [*Harnett et al.*, 2005], and heavy ion and ion cyclotron effects of reconnection in the terrestrial magnetosphere [*Winglee*, 2004].

[10] The fluid components of the plasma are described by

$$\frac{\partial \rho_\alpha}{\partial t} + \nabla \cdot (\rho_\alpha V_\alpha) = 0 \tag{1}$$

$$\rho_\alpha \frac{dV_\alpha}{dt} = q_\alpha n_\alpha [\boldsymbol{E} + \boldsymbol{V}_\alpha \times \boldsymbol{B}(\boldsymbol{r})] - \nabla P_\alpha - \left(\frac{GM_T}{R_T^2}\right)\rho_\alpha \vec{\boldsymbol{r}}, \tag{2}$$

$$\frac{\partial P_\alpha}{\partial t} = -\gamma \nabla \cdot (P_\alpha V_\alpha) + (\gamma - 1) V_\alpha \cdot \nabla P_\alpha, \tag{3}$$

where the subscript α denotes a particular fluid component of the plasma and M_T and R_T are the mass and radial distances from Titan. These equations are valid irrespective of the mass or charge of the fluid component. The multifluid treatment uses the same equations to advance the bulk moments of individual ion and electron species. As in the hybrid treatment, the multifluid method assumes the electrons are essentially massless. This approximation eliminates high-frequency plasma waves. Under this assumption (along with the assumption of quasi-neutrality), the electron momentum equation can be used to derive a modified Ohm's law that includes the Hall terms and the pressure gradient terms:

$$\vec{\boldsymbol{E}} \quad + \quad \vec{\boldsymbol{V}}_e \times \vec{\boldsymbol{B}} + \frac{\nabla P_e}{e n_e} = 0, \tag{4}$$

where

$$\frac{\partial P_e}{\partial t} = -\gamma \nabla \cdot \left(P_e \vec{\boldsymbol{V}}_e\right) + (\gamma - 1)\, \vec{\boldsymbol{V}_e} \cdot \nabla P_e \tag{5}$$

$$\vec{V}_e = \sum\nolimits_i \frac{n_i}{n_e} \vec{V}_i - \frac{\vec{J}}{e n_e},$$

and $\overrightarrow{J}$ is the current. The ionosphere was assumed to be fully conducting and no terms representing collision between ions are included. Independently modeling the ion and electron components of the plasma allows us to retain the Hall and pressure gradient term in the electric field equations. The Hall and electron pressure forces are responsible for flow-aligned electric field that can modify the overall magnetic topology and produce strong acceleration of ions in the presence of current sheets.

[11] The electric field equation in ideal or resistive MHD codes does not include these terms [*Ledvina and Cravens*, 1998; *Kabin et al.*, 1999; *Backes et al.*, 2005; *Ma et al.*, 2006]. These nonideal MHD corrections scale as the ration of the ion skip depth to the current sheet thickness. Therefore, in order to compare the multifluid results with MHD-like results simulations we ran two cases: (1) with the ratio of the ion skin depth to the grid spacing (125 km) set to its exact value (order unity) and (2) with the ratio of the ion skin depth set to much less than 1 to represent MHD-like conditions. The latter cases is not exactly ideal MHD since the electric field is explicitly carried in the momentum equation and an exact cancellation of nonideal MHD terms does not necessarily occur in the limit of small ion skin depth.

[12] Substituting the electric field equation into the fluid equation for momentum (equation (1)), we obtain the ion momentum equation

$$\rho_\alpha \frac{dv}{dt} = q_\alpha n_\alpha (\boldsymbol{v}_\alpha - \boldsymbol{V}_I) \times \boldsymbol{B}(\boldsymbol{r}) + q_\alpha \left(\frac{\boldsymbol{J} \times \boldsymbol{B}}{e n_e} - \frac{\nabla P_e}{e n_e} \right), \quad (6)$$

where

$$V_I = \sum_i \frac{n_i v_i}{n_e}.$$

[13] The magnetic field is advanced using the induction equation

$$\frac{\partial \overrightarrow{B}}{\partial t} = -\nabla \times \overrightarrow{E}. \quad (7)$$

The equations are solved on a nested grid system consisting of four boxes centered on Titan. The largest box extends 49 R_T along the x axis and 39 R_T in the y and z directions and has a resolution of 1215 km. The smallest box is centered at Titan and has a resolution of 125 km and extends 6 R_T in the x direction and 5 R_T in the y and z directions. Two intermediate boxes with resolutions of 245 km and 490 km are spaced between the smallest and largest box. The x coordinate is oriented in the direction of corotation, and the y coordinate is oriented toward Saturn. At each time step, information from the lower resolution boxes is passed outward to bordering higher resolution boxes at the corresponding resolution and results from outer boxes boarding lower resolution boxes are passed inward as boundary conditions. A second-order Runge-Kutta algorithm with a flux correction was used to solve for the plasma properties. Flux correction is required to remove unphysical grid point oscillations across sharp discontinuities such as the ionopause.

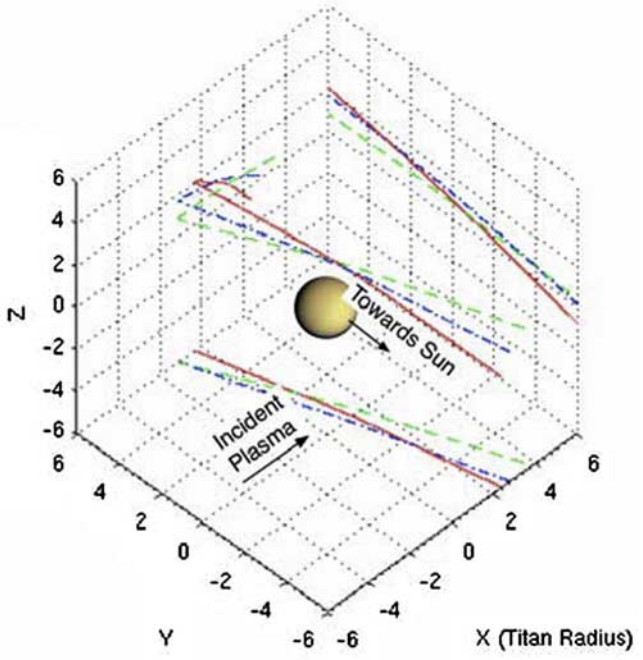

Figure 1. Geometry of the TA (red, solid), TB (blue, dash-dotted), and T3 (green, dashed) trajectories. The x axis points in the direction of incident plasma flow, and the y axis points in the direction of Saturn. The solar direction is indicated. The coordinate system shown is the same as the model coordinate system.

2.2. Initial Conditions

[14] The TA, TB, and T3 flybys (Figure 1) took place when Titan was at 10:36, 10:28, and 10:23 Saturn local time. Since each encounter took place in approximately the same place in Saturn's magnetosphere the incident field and plasma conditions were expected to be similar for each flyby. These encounters were designed in hopes of obtaining a very thorough description of the plasma interaction in a similar state [*Blanc et al.*, 2002].

[15] Kronian plasma and field conditions are introduced on the left hand boundary of the largest box. Table 1 list the Kronian magnetic field measurements near Titan during the inbound and outbound pass of each encounter. Values that gave the best fit for all three encounters were chosen for the Kronian magnetic field strength in our simulation. Cassini measurements of ion species during the TA flyby indicate that the dominant ions near the orbit of Titan are H^+, H_2^+, and O^+ [*Hartle et al.*, 2006]. Significant concentrations of nitrogen ions were not observed at Titan's orbital radius [*Young et al.*, 2005]. In our simulation the incident flow consisted of ions with a mass of 16 amu, for O^+, with a number density of 0.2 cm^{-3}.

[16] The flow parameters (Table 2) were chosen to match the magnetosphere conditions measured near Titan by Voyager 1. The flow speed is subsonic and super-Alfvenic with a speed of 120 km s^{-1} entirely in the x direction, $T_{16\ amu}$ of 4.6 keV, and a magnetic field of [1.8 nT, 2.4 nT, −4.9 nT].

Table 1. Kronian Field During TA, TB, and T3 Encounters

Flyby	B_{in}, nT	B_{out}, nT
TA	[2.0,3.8, −4.0]	[0.3,4.0, −5.6]
TB	[1.0,3.1, −3.0]	[1.7,2.1, −4.3]
T3	[−1.9,1.3, −3.9]	[0.627,2.8, −1.9]

Therefore the flow was subsonic (M_S = 0.57), super-Alfvenic (M_A = 1.7), and submagnetosonic (M_f = 0.54). Using Cassini plasma spectrometer and magnetometer measurements, *Ma et al.* [2006] estimated that the flow may have been supersonic, sub-Alfvenic, and submagnetosonic during TA and subsonic, sub-Alfvenic, and submangetosonic during TB. However, a bow shock was not observed during the TA encounter [*Backes et al.*, 2005]. It is also been suggested that the flow likely had significant components in the −y and z directions [*Ma et al.*, 2006; *Neubauer et al.*, 2006]. The intent of this study is not to perfectly match the conditions during the TA, TB, or T3 encounter but to develop a single model for all three encounters, which occurred at the same local time in Saturn's magnetosphere.

[17] During the T5 encounter, $HCNH^+$ was found to be the most abundant ionospheric species as predicted by most pre-Cassini models of Titan's ionosphere. The other abundant species measured were $C_2H_5^+$, CH_5^+, and $C_3H_5^+$ and heavy ion species $C_7H_7^+$ and $C_3H_3N^+$ [*Cravens et al.*, 2006]. The simulated ionosphere in our model includes a 28 amu ion species and a 1 amu ion species; this allows us to study the individual behavior of ion species with different masses. The density of the inner boundary of our model is 40 cm^{-3} for the heavy species (28 amu) and 200 cm^{-3} for light species (1 amu). The density of the ionosphere decays exponentially with a scale height of 700 km. The ion temperature on the inner boundary was initialized at 17 eV for the heavy component (28 amu) and0.5 eV for the light component (1 amu). The inner boundary has a radius of 1.1 R_T and the density of ionospheric plasma on the inner boundary is constant and uniform.

[18] Photoionization is the dominant ionization source [*Cravens et al.*, 1992; *Keller et al.*, 1998]. Therefore the most important factor that controls the density of the ramside ionosphere is solar zenith angle or Titan's position within Saturn's magnetosphere. The state of Titan's ionosphere during the TA, TB, and T3 encounters should have been very similar. The solar zenith angle was approximately 110° during the TA, TB, and T3 encounters; therefore the ramside ionosphere was only partially illuminated by the Sun. The solar zenith effect was accounted for in the simulated ionosphere with a peak density at the solar zenith point that decreases as a sinusoidal to the antisolar point.

3. Results

[19] In Figure 2 the magnetic field strength in the multifluid simulation along the TA, TB, and T3 trajectories is compared with Cassini magnetometer data. It has been shown that there was significant variation in the Kronian plasma density and magnetic field strength during the TA, TB, and T3 encounters [*Ma et al.*, 2006; *Neubauer et al.*, 2006]. For example, during the TA and T3 encounters the ambient Kronian magnetic field was significantly different before and after the Titan encounter. During the TB flyby the ambient field varied continuously during the Titan encounter. Despite these complications we find good agreement between the simulated and satellite data. The locations of magnetic pileup boundary (MPB) and ionopause boundary (IP), identified by rapid changes in the strength and orientation of the B_x magnetic field, correspond well with the Cassini observations. The spacecraft trajectories and the B_x magnetic field in a plane near the three encounters are shown in Figure 3. In the TA comparison crossings of the magnetic pileup boundary matches the Cassini data well. Also in the TA comparison we find our sample spacecraft does not cross the ionopause boundary even though the B_x field shifts from negative to positive before it exits the magnetotail. Instead we find the trajectory exits the northern magnetic lobe and entered a region of positive B_x that is due to kinking of the field lines on the Saturn-facing side (y direction in Figure 3) of Titan. The source of this kinking is the strong flow of the incident species into the magnetic cusp region that is located between the northern and southern magnetic lobes. In the TB and T3 comparisons the locations of the magnetic pile up boundaries in the TB and T3 comparison are reasonably well matched with Cassini data. In these encounters we find that the trajectory crosses the ionopause and enters Titan's ionosphere. In some regions, like in between the MBP and IP in the TB flyby and part of the T3 flyby, the strength of the magnetic field does not agree well magnetometer data. Improvement in the area may be obtained by fine tuning the incident velocity and density for each flyby.

[20] The large-scale morphology of the Titan interaction can be seen in Figure 4. The Kronian plasma has a very high conductivity and the magnetic field can be thought of as frozen into the flowing plasma. When the plasma flows near Titan the plasma that encounters Titan's ionosphere is slowed and the frozen-in field lines are forced to drape around the planet. The ambient Kronian plasma continues to flow past Titan and eventually the draped portion of the field line flow from the ram to wake side along the flanks of Titan's ionosphere. The significant B_x component of the magnetic field leads to particularly sharp bending above Titan's magnetotail and very gradual bending below the magnetotail.

[21] The importance of including ion gyroradius effects can be seen in the differences between the light and heavy ion tail. In Figure 4 isosurfaces at $10^{-1.7}$ cm^{-3} and $10^{-1.2}$ cm^{-2}

Table 2. Incident Flow Parameters

Incident Plasma Parameter	Simulated Value
Magnetic field B	[1.8 nT,2.4 nT, −4.9 nT]
Plasma flow speed ν	120 km s^{-1}
Mass m	16 amu
Mass density ρ	3.2 amu cm^{-3}
Temperature $kT_{16\ amu}$	4604 eV
Pressure P	1.5×10^{-10} N m^{-2}
Plasma beta β	11.6
Alfven speed c_A	69 km s^{-1}
Sonic speed c_S	210 km s^{-1}
Fast magnetosonic speed c_f	221 km s^{-1}
Alfven Mach number M_A	1.7
Sonic Mach number M_S	0.57
Magnetosonic Mach number M_f	0.54

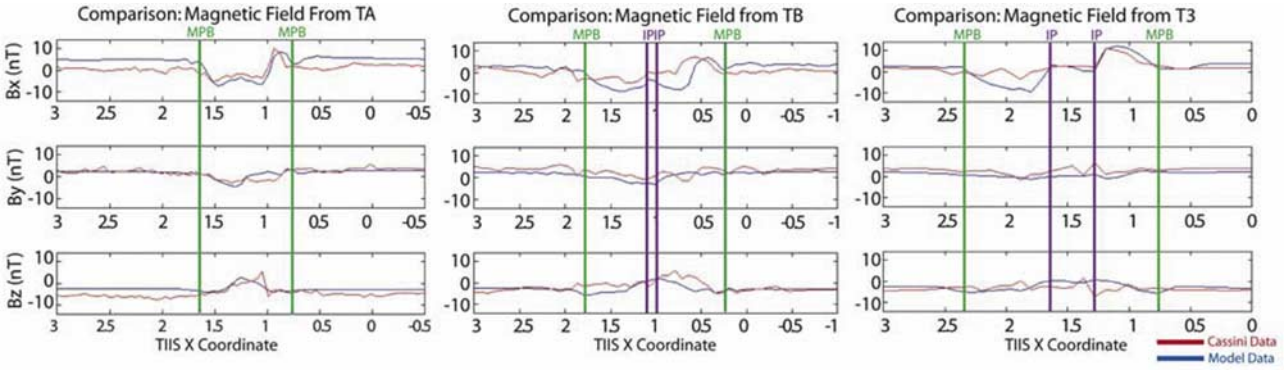

Figure 2. Magnetic field data from our simulation A (blue) is compared with Cassini magnetometer data (red) for the TA, TB, and T3 encounters. Each comparison is made from a simulation with identical incident and ionospheric conditions. Simulated ionopause (IP) and magnetic pileup boundary (MPB) crossing are marked.

are drawn to show the extent of Titan's ion tail. The light ion tail (1 amu) is much more symmetric than the heavy ion tail (28 amu). The difference in symmetry is due to the inclusion of ion gyroradius effects. The heavy ion isosurface of the near Titan ion tail shows a large inflated region on the anti-Saturn side (−y direction) of Titan that radially extends ∼3 R_T from the main ion tail before rejoining the ion tail about six ∼6 R_T downstream. The interaction of magnetic field lines with the inflated region causes more complex magnetic field draping. The magnetic field lines that do not wrap around Titan but instead interact with the heavy ion pick up region to be reversed draped. The reversed draped field lines are bent into an "S" shape giving positive values of B_x in regions where negative values would be expected and negative B_x values where positive values would be expected. In Figure 5 an example of this type of field line is highlighted in red. The draping of magnetic field lines is much more complex than ideal MHD diagrams depicting field lines symmetrically interacting with Titan.

[22] The asymmetric ion pickup process near Titan leads to asymmetries in the magnetic pileup and mass loaded region. Figure 6 displays Titan's ionosphere and induced magnetic field looking in the flow direction for a simulation

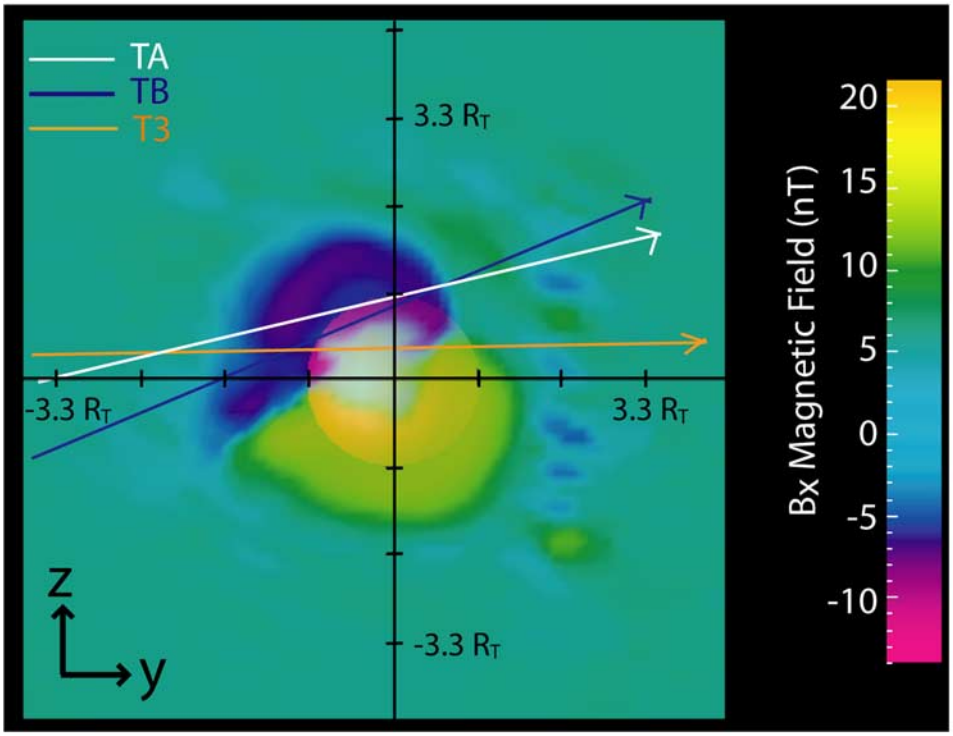

Figure 3. Magnitude of the B_x magnetic field near all three trajectories is plotted in the z plane from the perspective looking into the flow direction (−x direction). The TA, TB, and T3 trajectories through the simulated magnetotail are also shown.

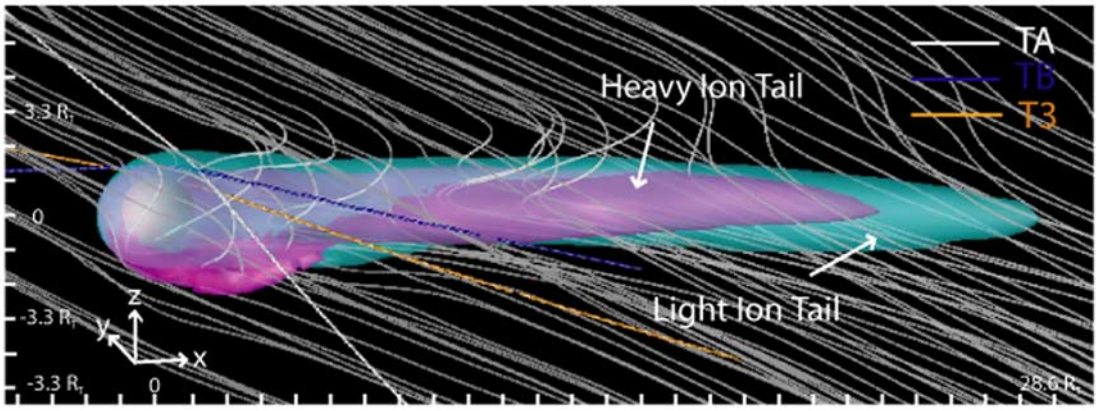

Figure 4. Magnetic field lines (shown in white) that interact with Titan's ionosphere, forming an asymmetric heavy ion tail (magenta) and a more symmetric light ion tail (blue). The heavy ion isosurface is drawn at a density of $10^{-1.7}$ cm^{-3}, and the light ion density is shown at $10^{-1.2}$ cm^{-3}.

that includes ion gyroradius effects (multifluid, right) and one that does not include ion gyroradius effects (MHD-like, left). Both show some bulging on the anti-Saturn side (−y direction) of Titan's ionosphere due to the solar effect; however, in the multifluid simulation the isosurface occurs at altitudes as much as 1000 km higher than in the MHD-like simulations.

[23] In both simulations the shape of the magnetic lobe isosurface generally follows the shape of the ionosphere isosurface. Therefore it is not unexpected that the magnetic lobe is also much more inflated on the anti-Saturn in the multifluid simulations. In MHD-like simulations the magnetic lobe is smaller and oval shaped which is consistent with results from recent MHD models [*Backes et al.*, 2005; *Neubauer et al.*, 2006]. Finally, in the multifluid simulations the spacing between the magnetic and the ionosphere isosurface is greater than in the MHD-like simulation. The ion cyclotron movement increases the thermal pressure within magnetic pileup region causing the magnetic pileup boundary to form at a higher altitude than in the simulation that does not include ion cyclotron terms.

[24] The dynamics of pickup ions in the near Titan environment also has a large impact on the heating of Titan's ionosphere by incident ions. In Figure 7 the heavy

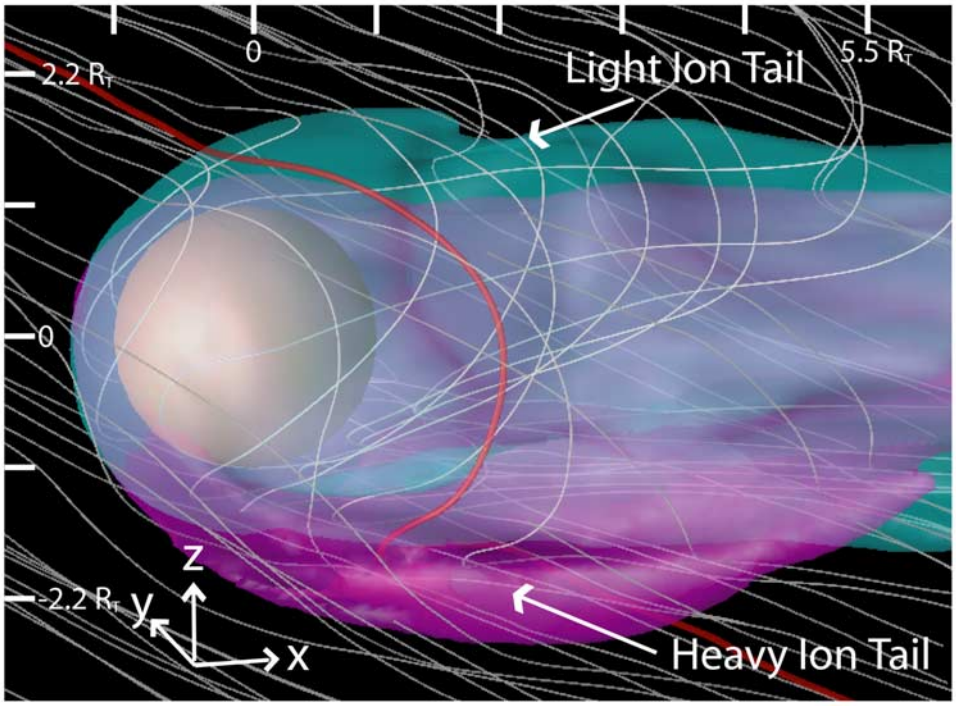

Figure 5. Magnetic field lines (shown in white) that interact with Titan's ionosphere. In the near-Titan region the heavy ion tail (magenta) is very asymmetric. Red highlights an example of a field line that is reversed draped. The heavy ion isosurface is drawn at a density of $10^{-1.7}$ cm^{-3}, and the light ion density is shown at $10^{-1.2}$ cm^{-3}.

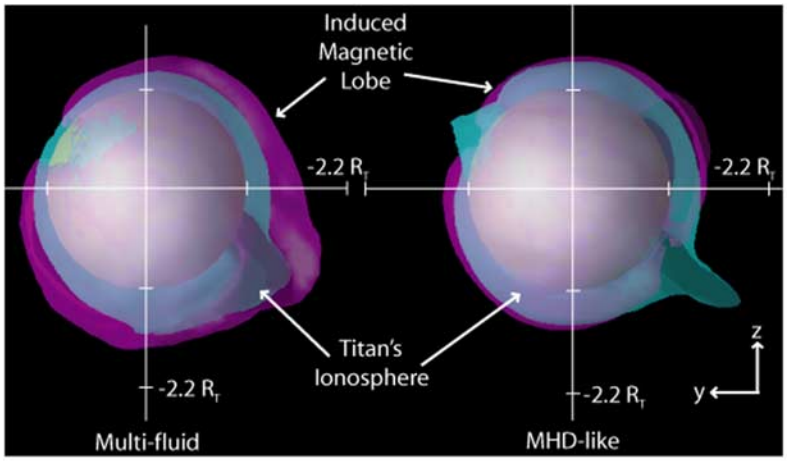

Figure 6. Comparison of an isosurface of Titan's induced magnetic lobe at 12 nT and an isosurface of the heavy ion density in Titan's ionosphere at $10^{-1.7}$ cm^{-3} for a model simulation that does not include ion gyroradius effects (MHD-like, right) and a model simulation that includes finite gyroradius effects (multifluid, left). The shape of the magnetic lobe generally follows the shaped of Titan's ionosphere. When ion effects are included, both the anti-Saturn side of the ionosphere and magnetic lobe are inflated.

ion temperature is mapped to a spherical surface at 1.5 R_T. Figures 7a and 7b display the heavy ion temperature in multifluid simulations while Figures 7c and 7d display the heavy ion temperature in MHD-like simulation. In the latter the heating of the anti-Saturn (Figure 7c) and Saturn side (Figure 7d) is similar and most of the ion heating occurs on the front side of the ionosphere, which is directly interacting with the incident flow. This result is very different from the multifluid result. On the anti-Saturn side ions are picked up from Titan's ionosphere inflating the mass loaded region and the magnetic lobe, as seen in Figure 6. The inflation creates a larger barrier for the incident plasma to penetrate and the shielding of Titan through currents that develop inside the ionosphere occurs at greater altitudes. The shielding of the high-energy incident plasma results in the anti-Saturn side of Titan's ionosphere having a lower temperature relative to the Saturn-facing side of the ionosphere at the same altitude.

[25] The Kronian $\vec{v} \times \vec{B}$ field also accelerates ions on the Saturn-facing side of Titan's ionosphere; however, their gyrorotation causes them to flow back into Titan's ionosphere instead of out into the Kronian magnetosphere. Therefore the ionosphere is not inflated on the Saturn-facing side of Titan's ionosphere and the shielding from ionospheric currents occurs at similar heights in the multifluid and MHD-like simulation (Figure 6). However, in the multifluid simulation the ions that are accelerated back into Titan's ionosphere by the $\vec{v} \times \vec{B}$ field on the Saturn-facing side are an additional source of energy for Titan's ionosphere. The size and shape of the magnetic lobe and mass

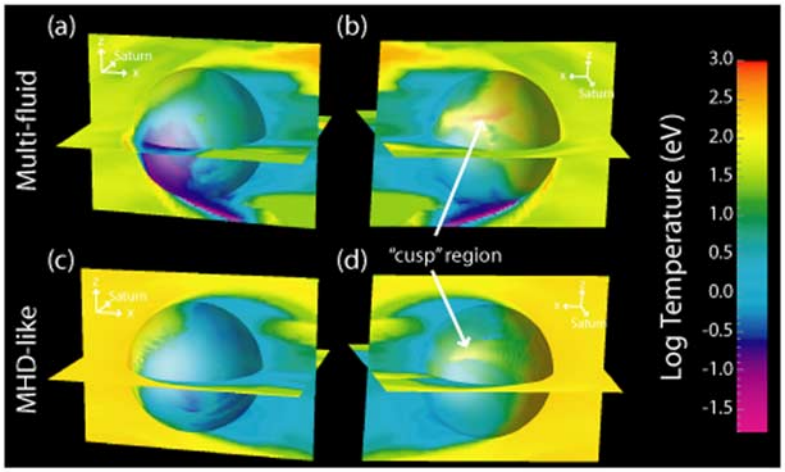

Figure 7. Heavy ion temperature mapped to 1.5 R_T and to y and z planes for (a) and (b) a model run including finite ion gyroradius effects (multifluid) and (c) and (d) a model run excluding ion gyroradius effect (MHD-like). The heating of the anti-Saturn (Figures 7a and 7c) and Saturn-facing sides (Figures 7b and 7d) of the ionosphere is much more asymmetric when ion gyroradius effects are included.

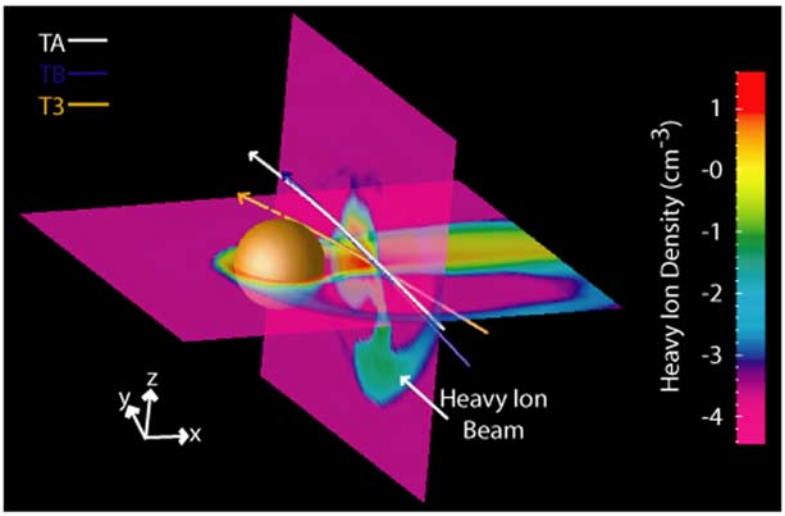

Figure 8. A cut of the heavy ion density in both the x and z planes, displaying the formation of ion beam on the anti-Saturn (−y) facing side of Titan's ionosphere.

loaded region are similar in Figures 7b and 7d; however, the heating is much greater in Figure 7b because of the acceleration and deposition of ionospheric ions. This could be an importance source of ion-neutral sputtering. The hottest spot on the Saturn-facing side of Titan's ionosphere is located in a cusp-like region between the two lobes where incident ions are accelerated into Titan's ionosphere. This is the same effect that caused the kinking of magnetic field lines described in the TA magnetic field comparison.

[26] Another important result of finite gyroradius effects is the formation of ion beams on the anti-Saturn side of Titan's ionosphere. The formation of ion beams was predicted by *Hartle et al.* [2006] and is the result of ions being picked up from Titan's ionosphere from the $\vec{v} \times \vec{B}$ electric field of the Kronian plasma. *Hartle et al.* [2006] noted that ions in Titan's exosphere have gyroradii that are much larger than the neutral gas scale heights and therefore are initially confined to a small portion of the possible velocity space. Therefore the picked ions form coherent beams in energy and space as they flow into the Kronian magnetosphere. Ion beams also develop in our multifluid simulations as seen in Figure 8. Once ions leave the region dominated by magnetic field draping they behave as ions freely gyrating in an ambient field and a coherent beam forms that resembles an arc with a radius equivalent to the gyroradii of the heavy ions in the ambient Kronian magnetic field (∼7000 km). The ions eventually collide with Titan's magnetotail about six Titan radii downstream and are incorporated into the wake of outflowing plasma. Ions within Titan's wake region are not accelerated away from the ion tail like they are in the near Titan region because the velocity distribution and field orientation causes them to be tightly confined to field lines that are parallel to the incident flow. Since ions in the backside of Titan's ionosphere do not experience ion beam formation a region of depleted heavy ions forms between the ion beam and the main ion tail. Our findings are very similar to the findings of *Ledvina et al.* [2000] whose study used a MHD electric and magnetic and field map to solve for single particle trajectories near Titan and in the wake region.

[27] The location of the bulk of the ion beam is determined by the direction of the incident field. For the initial conditions simulated the bulk of the ion beam formed well below the orbital plane. For this case Cassini would have flown above the densest portion of the ion beam during the TA, TB, and T3 encounters. This may be why a large asymmetric mass loaded region was not detected.

[28] The mass loss from Titan has been verified in situ by Cassini. Ion outflow along in the magnetotail and loss due to ion pickup from the anti-Saturn side of Titan's ionosphere are accounted for in the multifluid model. Ion-neutral sputtering is not included because we did not include neutral interactions in this simulation. By calculating ion flux through a surface surrounding Titan we calculated the total ion loss in our simulation to be 4×10^{25} s^{-1} which is on the same order as the ion loss rate measured by Cassini during the TA flyby, $\sim 10^{25}$ s^{-1} [*Wahlund et al.*, 2005].

4. Conclusions

[29] The results from our three dimensional multifluid simulation demonstrates that ion gyroradius and heavy ion effects cannot be neglected when characterizing the plasma interaction near Titan. Ion gyroradius and heavy ion effects drastically change the mass loading and magnetic field draping around Titan. The asymmetric pickup of ions from Titan's ionosphere leads to a very asymmetric mass loaded region. We find that the large ion gyroradius of picked up ionospheric species results in an extension of the ionosphere and therefore the mass loading and magnetic pileup on the anti-Saturn side of Titan. Also, the additional thermal pressure provided by heavy ion cyclotron motion in the near Titan causes the shielding currents to form at higher altitudes. The flow of energetic ions into Titan's ionosphere is also greatly affected by the inclusion of ion gyroradius effects. Ions on the anti-Saturn side of Titan's magnetosphere are accelerated away from Titan's into Saturn's magnetosphere; however, ions on the Saturn-facing side of Titan's are accelerated toward Titan and back into the ionosphere. Therefore the Saturn-facing side of Titan's

ionosphere experiences both less shielding from incident Kronian plasma and additional heating due to the acceleration of heavy ions in the ionosphere.

[30] Finally, ion gyroradius effects are also very important to the dynamics of ion outflow into the Kronian magnetosphere. We find that well-confined heavy ion beams form on the anti-Saturn side of Titan's magnetosphere and extends more than three Titan radii from Titan's main ion tail before rejoining the ion tail about six Titan radii downstream. The location of this ion beam is dependent on the Kronian field orientation and we find that during the TA, TB, and T3 encounters the bulk of the ion beam was located below Titan's equatorial plane. We also find good agreement with Cassini magnetometer data from the TA, TB, and T3 encounters and the ion loss rate measured by Cassini during the TA encounter for a single set of incident conditions.

[31] These results demonstrate that heavy ion and ion cyclotron effects change the size of the induced magnetosphere around Titan, the distribution of plasma within the induced magnetosphere, and the localized deposition of energy into Titan's upper atmosphere by pick up ions. The multifluid simulations also verify the formation of heavy ion beams that extend several Titan radii in to the Kronian magnetosphere.

[32] **Acknowledgments.** This work was supported by NASA grant NNG05GL9G to the University of Washington.

[33] Amitava Bhattacharjee thanks Christian Mazelle for his assistance in evaluating this paper.

References

Backes, H., et al. (2005), Titan's magnetic field signature during the first Cassini encounter, *Science*, *308*, 992–995.

Blanc, M., et al. (2002), Magnetospheric and plasma science with Cassini-Huygens, *Space Sci. Rev.*, *104*, 253–346, doi:10.1023/A:1023605110711.

Brecht, S. H., J. G. Luhmann, and D. J. Larson (2000), Simulation of the Saturnian magnetospheric interaction with Titan, *J. Geophys. Res.*, *105*, 13,119–13,130.

Cravens, T. E., C. N. Keller, and L. Gan (1992), The ionosphere of Titan and its interaction with Saturnian magnetospheric electrons, in *Proceedings of Symposium of Titan*, *Eur. Space Agency Spec. Publ., ESA SP-338*, 273–278.

Cravens, T. E., et al. (2006), Composition of Titan's ionosphere, *Geophys. Res. Lett.*, *33*, L07105, doi:10.1029/2005GL025575.

Harnett, E. M., and R. M. Winglee (2003), The influence of a mini-magnetopause on the magnetic pileup boundary at Mars, *Geophys. Res. Lett.*, *30*(20), 2074, doi:10.1029/2003GL017852.

Harnett, E. M., R. M. Winglee, and P. A. Delamere (2005), Three-dimensional multi-fluid simulations of Pluto's magnetosphere: A comparison to 3D hybrid simulations, *Geophys. Res. Lett.*, *32*, L19104, doi:10.1029/2005GL023178.

Hartle, R. E., et al. (2006), Preliminary interpretation of Titan plasma interaction as observed by the Cassini Plasma Spectrometer: Comparisons with Voyager 1, *Geophys. Res. Lett.*, *33*, L08201, doi:10.1029/2005GL024817.

Kabin, K., T. I. Gombosi, D. L. De Zeeuw, K. G. Powell, and P. L. Israelevich (1999), Interaction of the Saturnian magnetosphere with Titan: Results of a three-dimensional MHD simulation, *J. Geophys. Res.*, *104*, 2451–2458.

Keller, C. N., V. G. Anicich, and T. E. Cravens (1998), Model of Titan's ionosphere with detailed hydrocarbon ion chemistry, *Planet. Space Sci.*, *46*, 1157–1174.

Ledvina, S. A., and T. E. Cravens (1998), A three-dimensional MHD model of plasma flow around Titan, *Planet. Space Sci.*, *46*, 1175–1191.

Ledvina, S. A., T. E. Cravens, A. Salman, and K. Kecskemety (2000), Ion trajectories in Saturn's magnetosphere near Titan, *Adv. Space Res.*, *26*, 1691–1695.

Ma, Y., A. F. Nagy, T. E. Cravens, I. V. Sokolov, K. C. Hansen, J.-E. Wahlund, F. J. Crary, A. J. Coates, and M. K. Dougherty (2006), Comparisons between MHD model calculations and observations of Cassini flybys of Titan, *J. Geophys. Res.*, *111*, A05207, doi:10.1029/2005JA011481.

Neubauer, F. M., et al. (2006), Titan's near magnetotail from magnetic field and electron plasma observations and modeling: Cassini flybys TA, TB, and T3, *J. Geophys. Res.*, *111*, A10220, doi:10.1029/2006JA011676.

Paty, C., and R. Winglee (2004), Multi-fluid simulations of Ganymede's magnetosphere, *Geophys. Res. Lett.*, *31*, L24806, doi:10.1029/2004GL021220.

Sillanpää, I., E. Kallio, P. Janhunen, W. Schmidt, K. Mursula, J. Vilppola, and P. Tanskanen (2006), Hybrid simulation study of ion escape at Titan for different orbital positions, *Adv. Space Res.*, *38*(4), 799–805.

Sittler, E. C., Jr., R. E. Hartle, A. F. Viñas, R. E. Johnson, H. T. Smith, and I. Mueller-Wodarg (2005), Titan interaction with Saturn's magnetosphere: Voyager 1 results revisited, *J. Geophys. Res.*, *110*, A09302, doi:10.1029/2004JA010759.

Wahlund, J.-E., et al. (2005), Cassini measurements of cold plasma in the ionosphere of Titan, *Science*, *308*, 986–989.

Winglee, R. M. (2004), Ion cyclotron and heavy ion effects on reconnection in a global magnetotail, *J. Geophys. Res.*, *109*, A09206, doi:10.1029/2004JA010385.

Wolf, D. A., and F. M. Neubauer (1982), Titan's highly variable plasma environment, *J. Geophys. Res.*, *87*, 881–885.

Young, J., et al. (2005), Composition and dynamics of plasma in Saturn's magnetosphere, *Science*, *307*, 1262–1266.

C. Bertucci and M. Dougherty, Space and Atmospheric Physics Group, The Blackett Laboratory, Prince Consort Road, London SW7 2BZ, UK.

D. Snowden and R. Winglee, Department of Earth and Space Sciences, University of Washington, Box 351310, Seattle, WA 98195-1310, USA. (dsnowden@u.washington.edu)